Spring 2010

Characterization of the neutron flux spectrum at the Missouri University of Science and Technology Research Reactor

Zachary Andrew Kulage

Department:

CHARACTERIZATION OF THE NEUTRON FLUX SPECTRUM AT THE MISSOURI UNIVERSITY OF SCIENCE AND TECHNOLOGY RESEARCH REACTOR

by

ZACHARY ANDREW KULAGE

A THESIS

Presented to the Faculty of the Graduate School of the

MISSOURI UNIVERSITY OF SCIENCE AND TECHNOLOGY

In Partial Fulfillment of the Requirements for the Degree

MASTER OF SCIENCE IN NUCLEAR ENGINEERING

2010

Approved by

Gary E. Mueller, Advisor
Shoaib Usman
Arvind Kumar

PUBLICATION THESIS OPTION

This thesis consists of the journal article that will be submitted for publication to Nuclear Engineering & Design Journal. Pages 1-42 of this thesis have been prepared in the style utilized by the Nuclear Engineering & Design Journal.

ABSTRACT

A new remotely accessible shielded cell is being constructed at the Missouri University of Science and Technology Research Reactor (MSTR). The heavily shielded cell will be able to receive highly irradiated specimens directly from the reactor and will be equipped with radiation-hardened cameras, remote manipulators and gamma spectroscopy. The cell will allow the manipulation and monitoring of highly activated specimens from both a workstation at the MSTR and at remote locations using a Web-based internet interface. The ability to access and control the shielded cell via a remote internet connection will make it useful to a wide variety of users. Samples will be transferred to and from the cell using a pneumatic rabbit system that is directly attached to the nuclear reactor core. In support of the shielded cell the neutron spectrum has been measured using foil flux monitors. Multiple foils were irradiated and iterative runs were completed using the SAND-II program. An MCNP model was also developed to provide an approximate neutron flux spectrum to serve as an initial estimate for the SAND-II least squares fitting technique. The results showed a strong agreement in the thermal neutron energy region. Thermal, intermediate, and fast neutron full power fluxes for the MSTR were respectively calculated to be 2.94E+12 ± 1.9E+10, 1.86E+12 ± 3.7E+10 , and 2.65E+12 ± 3.0E+3 neutrons per square centimeter per second. The total neutron flux was calculated to be 7.55E+12 ± 5.7E+10 neutrons per square centimeter per second.

ACKNOWLEDGEMENTS

I wish to express my heartfelt gratitude and deep appreciation to Dr. Gary Mueller, my advisor, who guided me through many years of learning and always reminded me to look at the bigger picture, both in science and other endeavors.

I would also like to thank my committee members, Dr. Arvind Kumar, for his wisdom and experience, and Dr. Shoaib Usman, for his insights into matters I had not considered, and to all members for their support and cooperation. Special thanks to Mrs. Sheila Johnson and Ms. Roberta Cox for checking all necessary paperwork for errors and guiding me through the administrative jungle. Funding for this work was made possible by the Missouri S&T Chancellor's Fellowship Program.

I would like to thank the staff of the Missouri S&T nuclear reactor facility for allowing extensive access to the reactor and great support throughout many years both before and during this work. Gratitude is expressed to Mr. Bill Bonzer, Reactor Manager, for teaching myself and all students how a nuclear reactor operates, and also to Dan Estel for his inspirational attitude of lifelong learning.

Most importantly, I would like to thank my family who worked hard to make things possible for me that were not possible for them and also Stephanie Hurtado for never allowing me to give up; without them none of this would have been possible.

TABLE OF CONTENTS

LIST OF ILLUSTRATIONS

LIST OF TABLES

PAPER

Characterization of the neutron flux spectrum at the Missouri University of Science and Technology Research Reactor

Zak Kulage, Gary Mueller[1], Shoaib Usman[2]

A new remotely accessible shielded cell is being constructed at the Missouri University of Science and Technology Research Reactor (MSTR). The heavily shielded cell will be able to receive highly irradiated specimens directly from the reactor and will be equipped with radiation-hardened cameras, remote manipulators and gamma spectroscopy. The cell will allow the manipulation and monitoring of highly activated specimens from both a workstation at the MSTR and at remote locations using a Web-based internet interface. The ability to access and control the shielded cell via a remote internet connection will make it useful to a wide variety of users. Samples will be transferred to and from the cell using a pneumatic rabbit system that is directly attached to the nuclear reactor core. In support of the shielded cell the neutron spectrum has been measured using foil flux monitors. Multiple foils were irradiated and iterative runs were completed using the SAND-II program. An MCNP model was also developed to provide an approximate neutron flux spectrum to serve as an initial estimate for the SAND-II least squares fitting technique. The results showed a strong agreement in the thermal neutron energy region. Thermal, intermediate, and fast neutron full power fluxes for the MSTR were respectively calculated to be 2.94E+12 ± 1.9E+10, 1.86E+12 ± 3.7E+10 , and 2.65E+12 ± 3.0E+3 neutrons per square centimeter per second. The total neutron flux was calculated to be 7.55E+12 ± 5.7E+10 neutrons per square centimeter per second.

Keywords: SAND-II; flux spectrum unfolding; neutron flux measurement

1 Corresponding Author: Gary Mueller, Associate Professor of Nuclear Engineering, Missouri University of Science and Technology, 203 Fulton Hall, 300 W. 13th St., Rolla, MO, 65409; Phone: (573) 341-4348; email: gmueller@mst.edu

2 Corresponding Author: Shoaib Usman, Associate Professor of Nuclear Engineering, Missouri University of Science and Technology, 225 Fulton Hall, 300 W. 13th St., Rolla, MO, 65409; Phone: (573) 341-4745; Fax: (573) 341-6309; email: usmans@mst.edu

1. Introduction

The Missouri University of Science and Technology (Missouri S&T) has a 200 kW pool type light water moderated research reactor for educational use. The Missouri S&T reactor (MSTR) uses materials-test-reactor (MTR) type fuel. Training and education of students is conducted at the reactor along with various experiments including neutron activation analysis of irradiated materials. The reactor core includes a rabbit system with two irradiation locations. A bare rabbit tube allows maximum flux through a stainless steel tube while a cadmium rabbit tube is identical except for location and an extra cadmium lining to harden the neutron flux spectrum. Other irradiation facilities include a beam port and a core access element to allow dry irradiation of samples on a string.

Initial reactor criticality took place on December 9, 1961 under license R-79 (UMRR, 2008) at a level of 10 kW and the reactor was upgraded to the present day full power level of 200 kW in 1967. As shown in Fig. 1, there are fourteen low enriched uranium (LEU) fuel elements in an open pool heterogeneous reactor system with three stainless steel shim/safety control rods containing 1.5% natural boron for course reactor power control and one stainless steel regulating control rod to maintain steady state reactor power with fine control. A Pu-Be neutron source can be placed in a source holder tube near the core for reactor startup. The MSTR provides an important research and development role in the Global Nuclear Energy Partnership (GNEP) and can perform a number of diverse irradiation tasks. To enhance these capabilities, an internet-accessible heavily shielded cell (HSC) is being built at the MSTR. Through the web-based interface, a remote user will have access to a robotic sample manipulation system, video imaging inside the HSC, and a gamma spectroscopy system for analyzing a wide variety of highly irradiated specimens.

The initial fuel enrichment of the reactor was high enriched uranium (HEU) until the reactor was refueled in July of 1992 using low enriched uranium (LEU). Research reactors around the world have replaced HEU fuel with LEU fuel to prevent proliferation of special nuclear material. The Nuclear Regulatory Commission has defined low enriched uranium (LEU) as fuel containing less than 20% ^{235}U, while high enriched uranium (HEU) is comprised of fuel containing more than 20% ^{235}U. The United States Department of Energy replaces HEU fuel in research reactors with LEU fuel where possible to eliminate HEU from the civilian fuel cycle for non-proliferation purposes. The physical fuel for the MSTR is in the form of 0.51mm thick U_3Si_2-Al clad in 0.38mm thick aluminum. The present LEU core and previous HEU core are shown together in Fig. 1. All HEU fuel on site was replaced with LEU fuel. The fresh LEU core did not need the same number of fuel elements as the previous HEU core so position C3 was left blank.

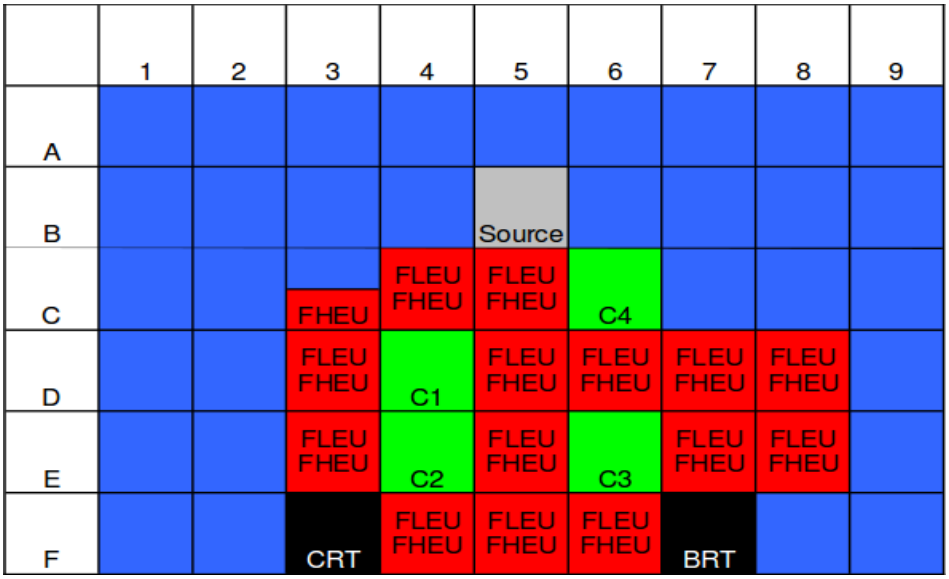

Fig. 1. Core configurations of the MSTR.

After the reactor was refueled with LEU fuel, the thermal and resonance neutron fluxes were determined using activation of gold foils by Khouaja (1995). Bare gold foils and cadmium covered gold foils were irradiated at various positions in the reactor, including the beam port. Cadmium covers were used to absorb thermal neutrons, allowing for irradiation from high energy fast neutrons while minimizing the contribution of thermal neutron activation. This method produced two group neutron fluxes of thermal and epithermal flux in the bare rabbit and cadmium rabbit tubes and the beam port location.

Some scientific applications require a more precise knowledge of the neutron spectrum than only the thermal and epithermal flux values can provide. Neutron activation analysis involves the irradiation of materials to probe into their elemental and isotopic makeup. Some stable isotopes can accept the absorption of a neutron and become a radioactive isotope. Radioisotopes have a characteristic half-life and will also emit gamma radiation at discrete energies. These discrete clues lead to the identification of radioisotopes with minimal error. Beyond identification of the presence of an isotope, neutron activation analysis can also provide the mass or concentration. Comparative techniques can be used when one known sample is analyzed and compared to the unknown. The obvious drawback to this technique is that a known sample must be present. Known samples are not always available for a variety of reasons, such as exotic isotopes that are in short supply or unavailable because of economic reasons. Neutron activation analysis is used to identify historical artifacts where preservation of the original source is paramount. Parametric techniques do not need an additional known sample. Concentration or mass of the radioisotope is derived from the number and energy of the neutrons that are bombarding the sample. It only stands to reason that more detailed information about the energy of the neutron field will add to the mass or

concentration accuracy of the radioisotope. Knowledge of the yield is central to the production and sale of radioisotopes as the quantity must be known with a small tolerance for error. Radiopharmaceuticals created in neutron fields of reactors are one such example of products under strict regulations as they must be sufficiently safe for human use. The MSTR is planning to increase radioisotope production, and research into methods of production of these isotopes would benefit from an enhanced neutron flux spectrum. Knowing the flux is also important from a safety standpoint when making radioisotopes, especially when predicting the activity of isotopes with high specific activity. The expected activity of a sample is calculated during a safety analysis of proposed experiments at the MSTR. Knowing the amount of expected radioactivity is the first line of defense against radiation exposure. Isotopes with higher activities than expected may unexpectedly fall into a higher regulatory category causing unnecessary disposal costs. Samples reading greater than 1 mSv/hr at a distance of 30 centimeters are required to have a health physicist present for sample handling for safety. If the sample is unexpectedly higher than the prescribed limit the health physicist must be summoned, which may be inconvenient. By careful calculation the activity of samples can be controlled to reduce safety concerns, regulatory issues, and overall exposure to persons handling the samples.

The HSC facility is being designed and constructed for use in the MSTR (Grant, 2010). The new cell is intended to be used for samples of higher activity. At the center of this cell system is a G-16 Roll Top Counting Shield from Gamma Products, Inc. The cell in being constructed in the basement of the reactor facility to minimize exposure to personnel, while also being equipped with an array of sensors and tools for remote analyzation and handling of the samples. Radiation-hardened cameras will allow visual inspection of samples while remote manipulators will allow sample handling from a

workstation located in the MSTR. Samples will travel directly to the reactor core using a pneumatic rabbit system. Detector ports will allow for multiple Geiger-Müller tubes as well as multiple High Purity Germanium (HPGe) detectors for gamma spectroscopy. The flexibility and versatility of the HSC lends well to the ability to easily upgrade and change detector systems in the future or to accommodate various measurement regimes. To set it apart from other similar systems, it will be equipped with a web-based interface to allow control and monitoring from a remote location and also to promote education in the field of radiation measurement and detection to schools and universities that are unable to easily access a nuclear research reactor. The HSC will benefit greatly from quantification of the neutron flux spectrum in the MSTR.

Neutron flux is usually non uniform throughout a reactor core. By measuring the neutron spectrum throughout the axial and radial planes of the core, enrichment can be tailored to produce the most economical conditions for fuel usage. Additionally, reactors with high volumetric power densities are required to ensure that no fuel assembly provides a disproportionate amount of power or exceeds the design limit. While thermocouples are a good tool to measure average water temperature in and around a fuel assembly, neutron flux measurements can provide additional or alternative techniques to measure power distribution throughout a reactor core. The MSTR is fortunate to not require specialized enrichment as the small core provides an even neutron flux across the core. Rearrangement of the fuel requires only minor changes in calibration of the instrumentation. High volumetric power density is not a concern for the MSTR due to the low overall maximum power level and a large temperature safety margin necessitating only natural convective cooling as is typical with relatively low power research reactors. Larger commercial nuclear power plants do have high volumetric power densities in order to maximize the amount of energy produced. These reactors also require

differential enrichment of the nuclear fuel to maximize fuel usage. A small percentage increase in fuel savings translates to substantial monetary gain as commercial nuclear reactors sell electricity in wholesale quantities.

The MSTR currently uses a power calibration technique whereby the thermal expansion of the pool water during reactor operation is correlated to reactor power. The increased pool water level caused by thermal expansion of the water is measured after the reactor has been operating. The water level is compared to the extrapolated water level as if the reactor were shutdown and the water were to evaporate under normal conditions. The difference between these levels reveals the energy produced by the reactor. Instrumentation is then calibrated to match the stated energy output. A drawback to this method is that barometric pressure must remain constant throughout the entire process as the evaporative water level is extrapolated from a point in time before the reactor begins operations which is on the order of a few hours. If the pressure changes significantly during any part of the process the extrapolated evaporative water level will be incorrect and the entire process must be repeated. The reactor must be shut down and the pool allowed ample time to cool to ambient temperature before the reactor may be restarted for the process. When a calibration cycle is believed to be accurate without a change in barometric pressure occurring, the process must be repeated multiple times to show consistent calibration data before the instrumentation is calibrated. Each calibration cycle takes at least one day and prevents any other reactor operations from taking place until full calibration is complete. A process that measures the neutron flux instead of pool water level for calibration would require less downtime for the reactor. Irradiated samples can be analyzed quickly after collection and the reactor may be used for other purposes during analysis. The calibration data may also be used to show trends from calibration to calibration as the neutron flux is absolute with little variation due to pool

water temperature. Pool water level and barometric pressure are not constant and do not trend as easily from calibration cycle to calibration cycle.

High energy neutrons have been known to cause material damage to the core structure and supporting apparatus in commercial nuclear reactors. Neutron flux measurements with high energy resolution are important to gain an understanding of the extent of the damage to the material and changing physical and material properties as the reactor ages. Damage assessments become important during relicensing of aging reactors because material properties usually change from ductile to brittle with high energy neutron damage. The core integrity must be such that the reasonable event of a control rod dropping quickly into the core during a scram would not breach the cladding of the fuel and release radioactive fission products outside of the core. Safety evaluations taking credit for ductility must be reevaluated during the relicensing process so that a more brittle irradiated material can withstand the tensile stresses associated with an accident scenario. The operating license for the MSTR was renewed in March of 2009 (Nguyen, 2009) and it was found that the low flux of the reactor was not sufficient enough to cause damage over the lifetime of the reactor to either the core structure or the fuel cladding. The MSTR contains a significant amount of aluminum 6061 in the core support structure. Aluminum is known to become brittle over time due to the activation of ^{27}Al and subsequent beta decay of ^{28}Al to the more brittle ^{28}Si. By knowing the neutron flux and energy of such flux, a correct assumption can be made as to the amount of silicon present in the core structure and the embrittlement that has occurred with a higher neutron flux. If a power uprate were to be requested for the MSTR at a future time an assessment reviewing the heightened flux would need to be completed. A narrower margin of error in the calculation of silicon production would allow a higher uprate power and increased flux availability for research.

2. Methodology

The general equation for predicting activity (McElroy et al., 1967) of a sample directly after irradiation is

$$A(t) = N\sigma\phi(1-e^{-\lambda t_i}) \quad (1)$$

where A is expected activity of the sample, N is the number of target atoms of the activating isotope, σ is the microscopic cross-section, φ is the neutron flux, λ is the decay constant of the product isotope, and t_i is the irradiation time. The number of target atoms is calculated using Eq. (2).

$$N = \frac{N_A m}{A_w} \quad (2)$$

N_A is Avogadro's number, m is mass of the isotope to be activated, and A_w is the atomic weight of the isotope.

Eq. (1) is limited by the mono-energetic nature of the cross-section and flux terms. The corresponding two group activity equation would expand to the thermal and resonance components

$$A(t) = N(\sigma_t\phi_t + \sigma_r\phi_r)(1-e^{-\lambda t_i}) \quad (3)$$

Eq. (3) can be expanded infinitely as suggested by McElroy et al. (1967) to represent different energy groups to suit particular applications as shown in Eq. (4).

$$A(t) = N(\sigma_1\phi_1 + \sigma_2\phi_2 + ... + \sigma_n\phi_n)(1-e^{-\lambda t_i}) \quad (4)$$

In the multiple foil activation method, multiple samples are irradiated and the resulting radioactivity is determined using a detector. Multiple unknown neutron flux terms can be found with multiple known activities of irradiated samples by solving systems of equations. The initial activity of isotopes can be related to activity of the same isotope at a later time using Eq. (5) from Shultis and Faw (2002).

$$A(t) = A_0 e^{-\lambda t} \tag{5}$$

which is rearranged to produce Eq. (6).

$$A_0 = \frac{A(t)}{e^{-\lambda t}} \tag{6}$$

with A_0 representing activity of product nuclide at time of sample removal from core and A representing activity after decay time, t.

By combining Eq. (3) and Eq. (5) and adding a term to account for efficiency, Khouaja (1995) was able to produce Eq. (7) which was used to determine the net count rate from a particular radioactive product isotope.

$$S = \xi N \sigma \phi (1 - e^{-\lambda t_i}) e^{-\lambda t_w} \tag{7}$$

with S as the gamma peak area expressed in counts per second, N as number density of target nuclide, ξ as the absolute efficiency of the detector also taking into account geometry. Time of irradiation and time between irradiation and start of counting are represented by t_i and t_w respectively. Saturation activity of an irradiated isotope is presented by McElroy et al. (1967) as Eq. (8).

$$A_s = \frac{A(t)}{1 - e^{-\lambda t_i}} = N \sigma \phi \tag{8}$$

From Eq. (8) it is clear that saturation activity is a simple function of mass, cross-section, and neutron flux. This equation forms the basis of this study to determine energy dependent neutron flux through the use of energy dependent cross-section data, mass, and saturation activities of many different irradiated samples.

3. Foil selection and irradiation

Foils for irradiation were selected according to availability and cross-section spectrum. Since cross-section spectra are similar in shape for a given type of neutron interaction, it is generally not important to choose specific interactions based on foils. More specifically, it is important that there is a relatively high number and variety of different neutron reactions to provide an adequate amount of data. A list of foils used and corresponding neutron reactions can be found in Table 1. It is noteworthy that some foils are able to provide more than one reaction, such as iron, which has products that decay by alpha, proton, and gamma modes of decay. Half-life values were obtained from Baum et al. (2002). The cross-section spectra for the neutron reactions listed in Table 1 are shown in Fig 2.

Table 1. Foil reactions

Foil	Reaction	Half-life
Dysprosium	DY164(n,g)DY165	2.33 h
Indium	IN113(n,g)IN114M	49.51 d
Gold	AU197(n,g)AU198	2.6952 d
Copper	CU63(n,g)CU64	12.7 h
Aluminum	AL27(n,a)NA24	14.95 h
Cobalt	CO59(n,g)CO60	5.271 y
Silver	AG109(n,g)AG110M	246.76 d
Nickel	NI58(n,p)CO58	70.88 d
Nickel	NI64(n,g)NI65	2.517 h
Nickel	NI60(n,g)CO60	5.271 y
Iron	FE56(n,p)MN56	2.578 h
Iron	FE58(n,g)FE59	44.5 d
Iron	FE54(n,a)CR51	27.702 d
Iron	FE54(n,p)MN54	312.1 d

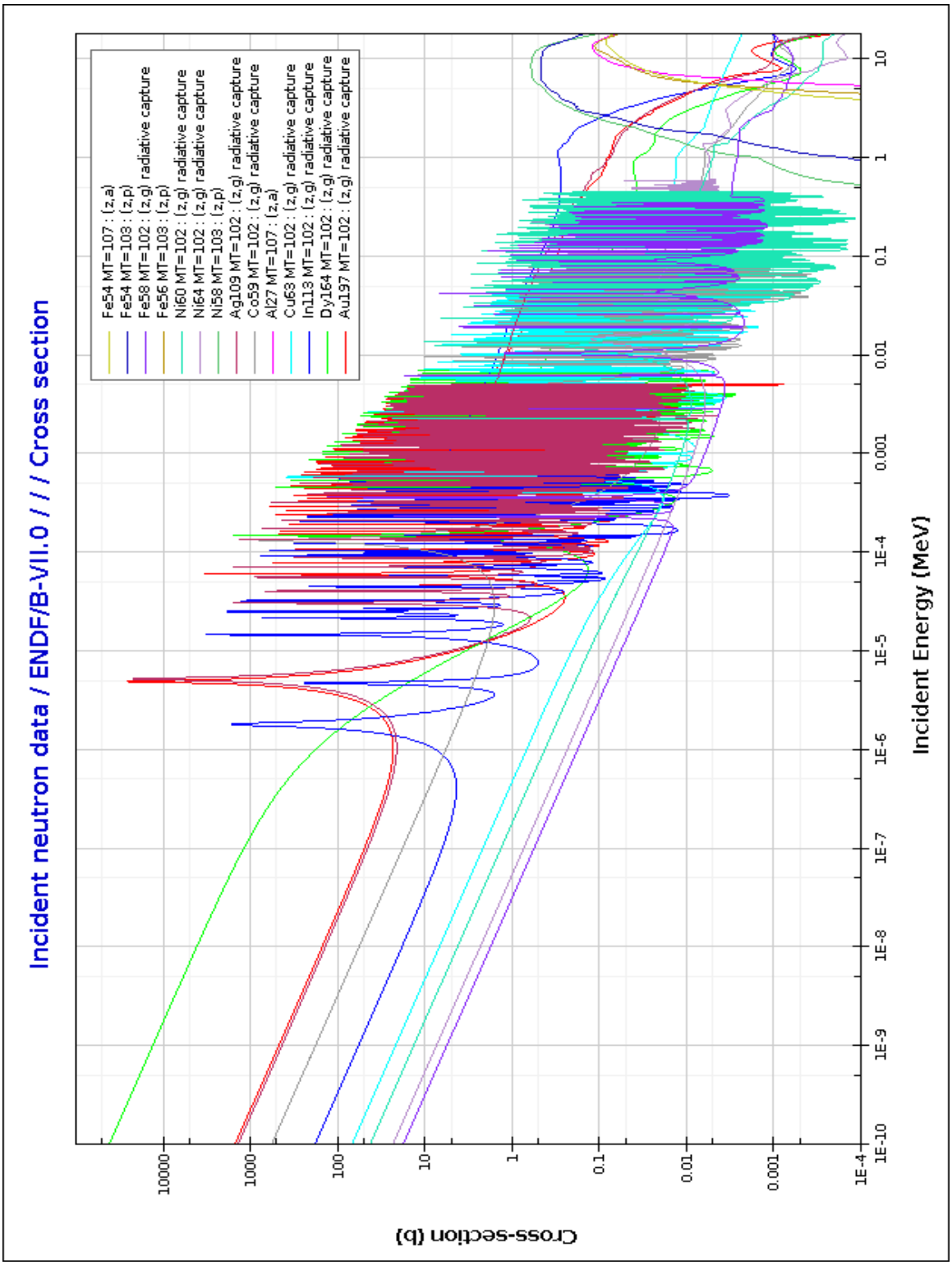

Fig. 2. Microscopic cross-section spectra of foil reactions.

As can be seen in Fig. 2, the microscopic cross-section for neutron reactions resulting in the release of a photon (n,γ) decrease as the energy of the neutron is increased. Neutron-gamma reactions tend to have a higher cross-section at low energy, followed by a resonance region, and a decreasing cross-section at high energies. Neutron-alpha (n,α) and neutron-proton (n,p) reactions have a threshold energy below which no reaction takes place. The threshold energy is dependent upon the minimum energy required to displace an alpha nuclei or proton from a particular isotope. These reactions are particularly useful for unveiling the high energy neutron flux as their cross-section makes them impervious to low energy neutron interactions.

Foils were prepared for activation in the MSTR according to expected activity. Foils with higher cross-sections had smaller mass to prevent unsafe levels of radiation during handling. Foils were irradiated in a polyethylene vial on a stringer placed in the source holder location for three minutes. The bolt passing through the center of the source holder tube at the core height mid-plane was used as a reference point. The irradiation location of the sample vial was located 12 inches above this reference point. One set of foils were irradiated at 200 kW and the other set at 100 kW. Each irradiation took place at the same bulk pool temperature of 76°F, according to two thermocouples located below and on opposite sides of the core. Samples were allowed to decay underwater until radiation levels were deemed safe for handling. Samples were counted using a high purity germanium detector (HPGe) connected to a multi channel analyzer with 16,384 channels and Genie-2000 acquisition software. Counting time was dependent upon the time scale of the half-life of the specific reaction being measured. Each foil was usually counted for one day except for foils with a short enough half-life to preclude counting for one day, in which case counting time was reduced to approximately 2 hours.

The HPGe detector was able to differentiate between isotopes with different half-lives allowing for multiple reactions to be counted using one foil. Foils with more than one reaction of interest were counted twice at different times if the half-lives were significantly different enough to warrant both long and short data acquisition. A short counting time of two hours was used to measure the short half-life and a long counting time of one day was later used to measure the longer half-lives. The primary reasons for this method were to optimize detector usage time directly after irradiation so that all short lived half-lives could be measured and also to reduce or completely eliminate the short lived half-life background during the counting of the longer lived half-lives.

The Genie-2000 software uses an algorithm to calculate saturation activity (Canberra, 1998) and the corresponding uncertainly of the value based upon the principles of Eq. (7) and Eq. (8). The saturation activity would represent the activity of the sample as if it had been irradiated for an infinite period of time with no material depletion in the sample. The specific saturation activity as calculated by the Genie-2000 software is given by Eq. (9).

$$C = \frac{S}{V \varepsilon' y T_1 U_f K_c K_w K_i} \tag{9}$$

where S is the net peak area, V is the sample mass, ε' is the attenuation corrected efficiency, y is the branching ratio of the peak energy, T_1 is the live time of the collection in seconds and U_f is a conversion factor for the software to internally convert between units of μCi and Bq. K_c is the correction factor for the nuclide decay during counting as shown in Eq. (10), K_w is the correction factor for the nuclide decay from the time the

sample was obtained to the start of counting as shown in Eq. (11), and K_i is the correction factor for sample irradiation time as shown in Eq. (12).

$$K_c = \frac{T_{1/2}}{\ln(2)t_c}\left[1 - e^{\frac{-\ln(2)t_c}{T_{1/2}}}\right] \tag{10}$$

where $T_{1/2}$ is the half-life of the nuclide and t_c is the elapsed clock time during the measurement.

$$K_w = e^{\frac{-\ln(2)t_w}{T_{1/2}}} \tag{11}$$

where t_w is the elapsed clock time from the time the sample was obtained to the beginning of counting.

$$K_i = 1 - e^{\frac{-\ln(2)t_i}{T_{1/2}}} \tag{12}$$

where t_i is the irradiation time of the sample. The random uncertainty of the saturation activity, C, is expressed in Eq. (13) from Canberra (1998).

$$\sigma_c = C\sqrt{\left(\frac{\sigma_R}{100}\right)^2 + \left(\frac{\sigma_S}{S}\right)^2 + \left(\frac{\sigma_V}{V}\right)^2 + \left(\frac{\sigma_{\varepsilon'}}{\varepsilon'}\right)^2 + \left(\frac{\sigma_y}{y}\right)^2 + \left(\frac{\sigma_K}{K}\right)^2} \tag{13}$$

where σ_R is the random uncertainty in percent, σ_S is the uncertainty of the total peak area S, σ_V is the uncertainty of the sample mass V, and $\sigma_{\varepsilon'}$ is the uncertainty of the effective efficiency of the system as shown in Eq. (14).

$$\sigma_{\varepsilon'} = \varepsilon \sqrt{\left(\frac{\sigma_{\varepsilon}}{\varepsilon}\right)^2 + (\rho t \sigma_{\mu(E)})^2 + (\mu(E)\sigma_{\rho t})^2} \tag{14}$$

where ε is the non-attenuation corrected detection efficiency, σ_ε is the uncertainty of the non-attenuation corrected detection efficiency, μ(E) is the mass attenuation (cm^2/g) at a gamma of energy E, $\sigma_{\mu(E)}$ is the corresponding uncertainty, ρτ is the average sample mass per area, $\sigma_{\rho t}$ is the corresponding uncertainty, σ_y is the uncertainty of the branching ratio y of the particular isotope being measured, and σ_K is the uncertainty of the composite decay correction factor, K as shown in Eq. (15).

$$\sigma_K = K \sqrt{\left(\frac{\sigma_{K_c}}{K_c}\right)^2 + \left(\frac{\sigma_{K_w}}{K_w}\right)^2 + \left(\frac{\sigma_{K_i}}{K_i}\right)^2} \tag{15}$$

where the composite decay correction factor K is defined in Eq. (16).

$$K = K_c K_w K_i \tag{16}$$

where K_c, K_w, and K_i are defined in Eq. (10), Eq. (11), and Eq. (12) respectively. The uncertainty values σ_{Kc}, σ_{Kw}, and σ_{Ki} are shown in Eq. (17), Eq. (18), and Eq. (19), respectively.

$$\sigma_{K_c} = \left(\frac{1 + K_c}{T_{1/2}}\right)\sigma_{T_{1/2}} \tag{17}$$

$$\sigma_{K_w} = \frac{K_w \ln(2) t_w}{(T_{1/2})^2}\sigma_{T_{1/2}} \tag{18}$$

$$\sigma_{K_i} = \frac{(1 - K_i)\ln(2) t_i}{(T_{1/2})^2}\sigma_{T_{1/2}} \tag{19}$$

The uncertainty values $\sigma_{T1/2}$ for half-life and σ_y for the branching ratio were taken from the Genie-2000 internal library of nuclides. If no value was present in the library for a value, it was set to zero in the cases of In-114m, Cu-64, and Ni-65.

The total uncertainty of the saturation activity as measured is determined by combining Eqs. (9-19) to form Eq. (20).

$$\sigma_{C(T)} = \sigma_C + \frac{\sigma_{sys} C}{100} \tag{20}$$

where σ_{sys} is the user defined systematic uncertainty.

The detector system was calibrated using a multi-isotope europium source consisting of Eu-152, Eu-154, and Eu-155. This check source was used because the range of gamma energy peaks emitted cover a broad spectrum of the HPGe energy range. The initial activity of the Eu source was also professionally determined to within 5%, which is the basis for the efficiency uncertainty to be set at 5%.

4. MCNP models

A model of the MSTR was formulated (King, 2009) using MCNP version 5. This model was used to simulate the neutron flux spectrum of the sample vial that the foils were placed in and to also serve as an initial guess for the SAND-II program as is described in section 5. The polyethylene vial was modeled to simulate a neutron environment as close as possible to the environment in which the foils were irradiated. Flux values were obtained using a track-length estimator tally (F4:N) from the space inside of the vial representing the effective flux received by irradiated samples. Fuel elements were modeled in heterogeneous plate form according to original shipping documents. The core structure was modeled using blueprints and available diagrams. Fuel composition was in the form as shipped and was individualized for each fuel element. The model does not take into account burnup of the fuel that has occurred. As of this study, no complete burnup analysis has been performed for the MSTR, however the spectrum obtained from the MCNP model still serves as a good initial guess for purposes of neutron flux spectrum analysis. The reactor will still have the same general neutron energy spectrum through burnup and variations of this spectrum can only be compared to measurements taken at the beginning of the core lifetime. Comparisons of detailed neutron spectra can only occur during the next core loading when more data is available. The problem was run in MCNP as a criticality eigenvalue problem (KCODE) with 1,000 simulated active cycles, 50 discarded cycles, and 20,000 particles per cycle. As MCNP reports all results in a normalized fashion, a flux multiplier was needed to obtain simulated spectra for full power and for half power. Eq. (21) is the first step to calculate this multiplier provided by the X-5 Monte Carlo team (2008).

$$\left(\frac{1J/g}{1W}\right)\left(\frac{1\,MeV}{1.602\times10^{-13}J}\right)\left(\frac{fission}{180\,MeV}\right)=3.467\times10^{10}\frac{fissions}{W-s} \quad (21)$$

The assumption in Eq. (21) is that the reactor is a uranium fueled reactor which is valid for the MSTR. The average number of neutrons produced per fission (ν) must also be known for correct calculation of the flux multiplier. An estimate for this number is found in the MCNP output file and was found to be 2.439 for the MSTR. Shultis and Faw (2002) put this number at 2.43 for thermal fission of ^{235}U and 2.57 for ^{238}U. As the majority of fissions of the fuel are occurring within the ^{235}U with a smaller contribution from ^{238}U, it does make sense that the simulated value would fall near yet slightly above that of ^{235}U. Using Eq. (22) (X-5, 2008) the multipliers in Table 2 were found.

$$M=3.467\times10^{10}\times\nu\times P \quad (22)$$

where P represents reactor power in Watts and M represents the flux multipler.

Table 2. Flux multiplier values for different power levels in the MSTR from Eq. (22)

Power (kW)	**Flux Multiplier**
100	8.456013E+15
200	1.691202E+16

To gain an additional source of thermal neutrons, the reactor core may be moved into close proximity to a graphite thermal column. This allows for greater neutron reflection, higher reactivity in the core, and increased thermal neutrons in the dry irradiation facility located in the graphite thermal column. Samples may be placed in multiple locations within the thermal column for irradiation with differing levels of graphite moderation and no contact with the reactor pool water. When the reactor is placed as close as possible to the thermal column it is considered in "T" or thermal mode. For this study and for the majority of normal reactor operations the reactor core is placed a fixed distance away from the thermal column in "W" or water mode allowing for optimal alignment with the beam port as seen in Fig 3.

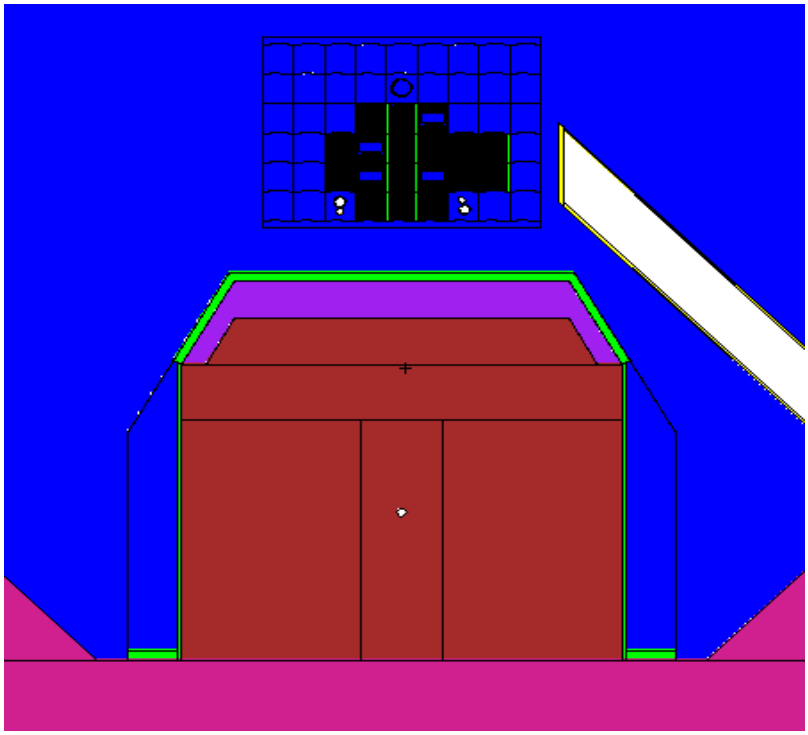

Fig. 3. MSTR core, thermal column, and beam port.

A closer view of the core is shown in Fig 4. The sample vial was placed in the source holder tube located in core position B5. The four control rod assemblies are located in positions C6, D4, E4, and E6. All use shim/safety control rods except for position C6, which contains the stainless steel regulating rod. Positions F3 and F7 contain the cadmium and bare rabbit tubes respectively. The larger diameter tubes in the rabbit system are used for the sample vial travel path. The smaller diameter tubes of the rabbit system are used as a flowpath for the nitrogen gas to provide the necessary pressure to remove the sample vial from the reactor. The tubes are connected at the lower section of the reactor core.

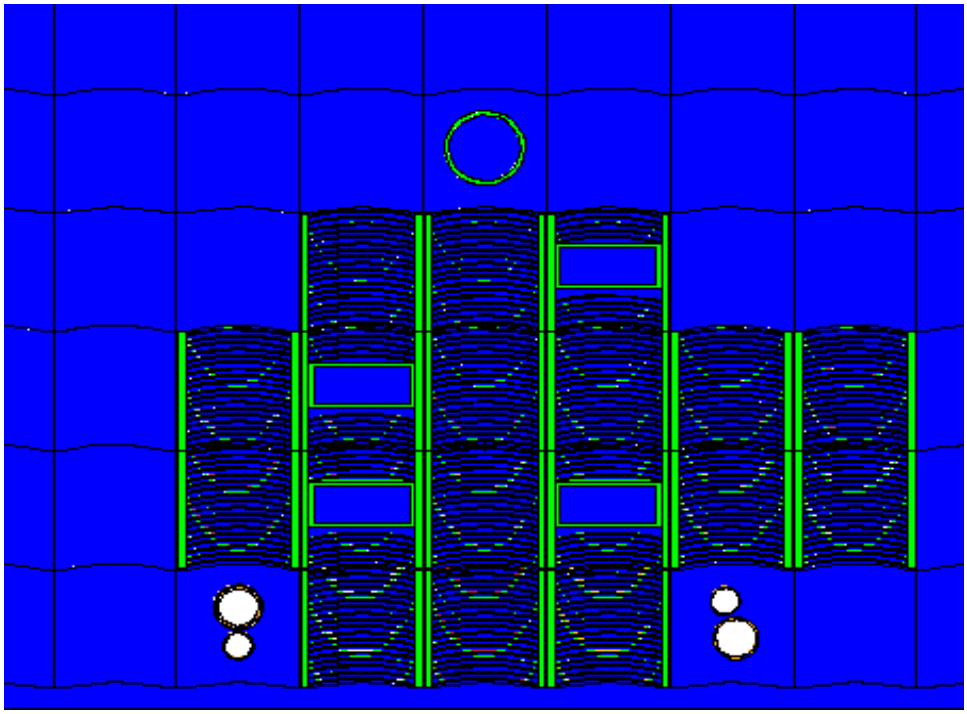

Fig. 4. MSTR core fuel, rabbit system, and source holder tube.

An MCNP simulation was also created to model all foils stacked together in a linear fashion. This simulation was run to test for the self shielding ability of all foils as a whole which is shown in Fig. 5 and the foil thicknesses as stated by the manufacturers are shown in Table 3. As all materials absorb neutrons even in minute quantities, a model was created to ensure that the absorption rate of the foil materials were not so great to alter the neutron flux itself. The list of foils in Table 3 corresponds to the placement in the model as shown in Fig. 5 from left to right. The figure is shown to give a reference as to the relative size of the foils to each other. The number of neutrons that successfully passed through all foils were counted and compared to the total number of neutrons simulated. The starting energy of the neutrons was isotropically sampled from the same fission spectrum as used in the full core MCNP model.

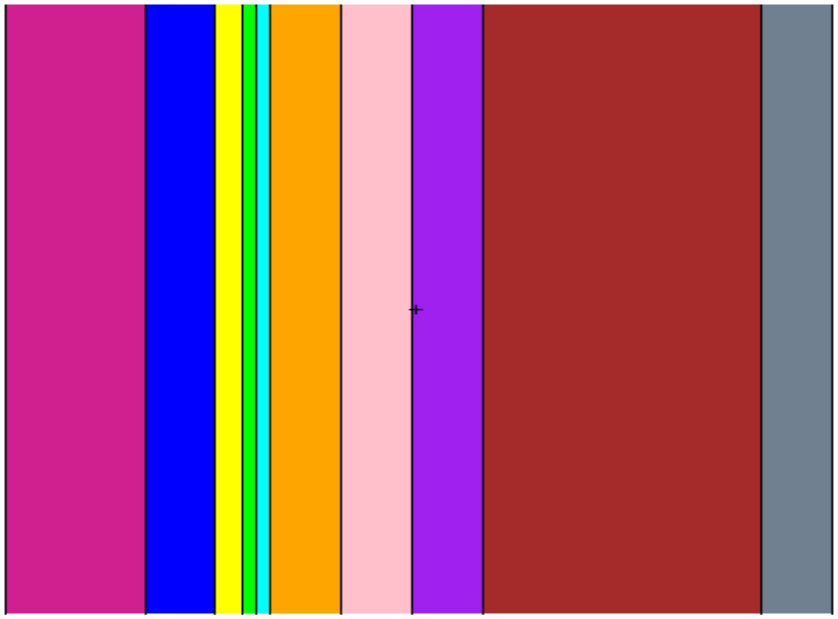

Fig. 5. Self shielding MCNP foil model.

Table 3. Foil thicknesses

Foil	**Thickness of foil (μm)**
Dy	250
V	127
In	50
Au	25
Cu	25
Al	127
Co	127
Ag	127
Ni	500
Fe	127

5. SAND-II model

The SAND-II program was developed by McElroy et al. (1967) for determination of neutron flux environments by the multi foil activation method utilizing Eq. (23).

$$A_s = m_0 \int_0^\infty \sigma_{mn}(E)\phi(E)\,dE \tag{23}$$

where

$$\phi(E) = \phi(E,t) \tag{24}$$

and t represents time. The foils must be irradiated in a constant flux field or at a steady state reactor power.

Upon inspection, Eq. (23) is merely the continuous integral expansion of Eq. (8) and can be formed from Eq. (4). By irradiating mulitple foils to obtain multiple saturation activities, a system of equations can be solved to obtain a solution to φ(E) due to the differences in cross-sections, σ(E), for different foils at different energies.

The code divides Eq. (23) into 620 discrete intervals of energy that range from 10^{-10} MeV to 18.0 MeV and 621 points to bound the intervals. This creates 621 unknown variables, namely the discrete flux values for each energy bin. To solve a system of linear equations, the number of equations must be equal to the number of unknowns. The number of equations is based upon the number of activated samples, more specifically, the number of identified reactions as shown in Table 1.

As the number of foils is much smaller than the number of unknown cross-sections, the problem does not have a unique solution. It must be solved by a least squares fitting technique based on an initial guess.

The initial estimate should be based on knowledge of the environment under study. As the solution will not necessarily be a unique one, a more accurate initial spectrum will yield a better representation of the true spectrum. The code provides a library of reference spectra available for use as an initial estimate but the ideal estimate would be based on the reactor environment itself using any available information.

The SAND-II program uses an internal library of cross-section information for calculation of the neutron flux spectrum. Each nuclear reaction has a specific entry in the library. The default format for cross-section entries is in the native SAND-II 620 group energy structure. Each decade between 10^{-10} and 1 MeV contains 45 intervals of equal width corresponding to 5 intervals in every integer of each decade. At energies above 1 MeV, each interval has a width of 100 keV. Cross-section entries in the library may be entered in a different format, which will be internally converted by the SAND-II program. The library used was created from ENDF-VII (Chadwick et al., 2006) cross-section data. The NJOY software program (MacFarlane and Muir, 1994) was used to format the cross-section data from the ENDF-VII files to the SAND-II 620 group structure for each reaction used in the study.

Foil activity information was combined with the results of the MCNP simulation of the reactor to create an input file for the SAND-II program. The least squares fitting technique is an iterative process using the MCNP simulated flux spectrum in the sample vial as an initial guess for the neutron flux spectrum. During each iteration the activities of the foils are calculated based upon the current iterative spectrum and compared to the measured activities of the foils. Correction factors are created for each foil and applied to the spectrum to bring the measured and calculated values closer. The new spectrum is used in the next iterative step and the process is repeated until the next iterative spectrum falls within a user defined difference of the previous spectrum or when a user set limit of

iterations has been achieved. These limits were designed to allow the user to choose the level of accuracy based on available computing time. As computers are much more powerful now than when SAND-II was written, the precision value was set to the lowest allowed value of 1% while the number of iterations was set to an arbitrarily high number of 5,000. This allowed the program to run as many iterations as needed until the spectrum differed by less than 1% of the preceding spectrum.

To take into account the uncertainty of the saturation activity values, a Fortran program was created to run SAND-II multiple times with differing activity values to produce a collection of spectra. The program ran SAND-II with no uncertainty in the activity values to obtain an "actual" spectrum. In the second and third runs all foil activities were set to their minimum and maximum values respectively including uncertainty. To completely know the extent to which the spectrum is affected by changes in foil activity every possible variation of foil activity and uncertainty would have to be run. The number of possibilities can be determined by Eq. (25) shown below

$$C_f = 3^F \tag{25}$$

where F is the number of foils and C_f is the number of combinations possible. For a set of 14 foil reactions, Eq. (25) would provide 4,782,969 possible combinations to run through SAND-II. As each combination must be iteratively run through the program, running all possible combinations is not feasible. Instead, 5,000 random combinations were used. After each iterative combination, a list of the lowest and highest flux values obtained thus far were revised if the iterative flux value was not between these values. This process was completed for both sets of full-power and half-power data. These values did not constitute a spectrum in and of themselves since they were merely a

patchwork of the highest and lowest flux values obtained. Instead they served as an estimate of the amount of error present in the study due to the effect of saturation activity uncertainty.

6. Results

It was found from the MCNP model that self shielding of the foils was not a concern. Of the 3.05 x 10^{10} neutrons that were simulated, 99.9845% were able to pass through all foils leaving an error in total flux of only 0.0155%, which is the fraction of neutrons that were absorbed or scattered by the foils. This was considered a low enough value to safely assume that self shielding between foils was negligible.

Fig. 6 and Fig. 7 show the MCNP simulated neutron flux spectrum, the actual spectrum obtained from SAND-II without the effect of uncertainty, and the maximum and minimum spectra values in each energy bin recorded for both full power and half power data. It is worth noting that while the maximum and minimum spectra may differ, the shape of the actual flux spectrum at full power and half power is generally consistent even though both spectra were created with different foil data. To do a more through comparison, differential and integral flux spectra were normalized to unity and plotted in Fig. 8 and Fig 9.

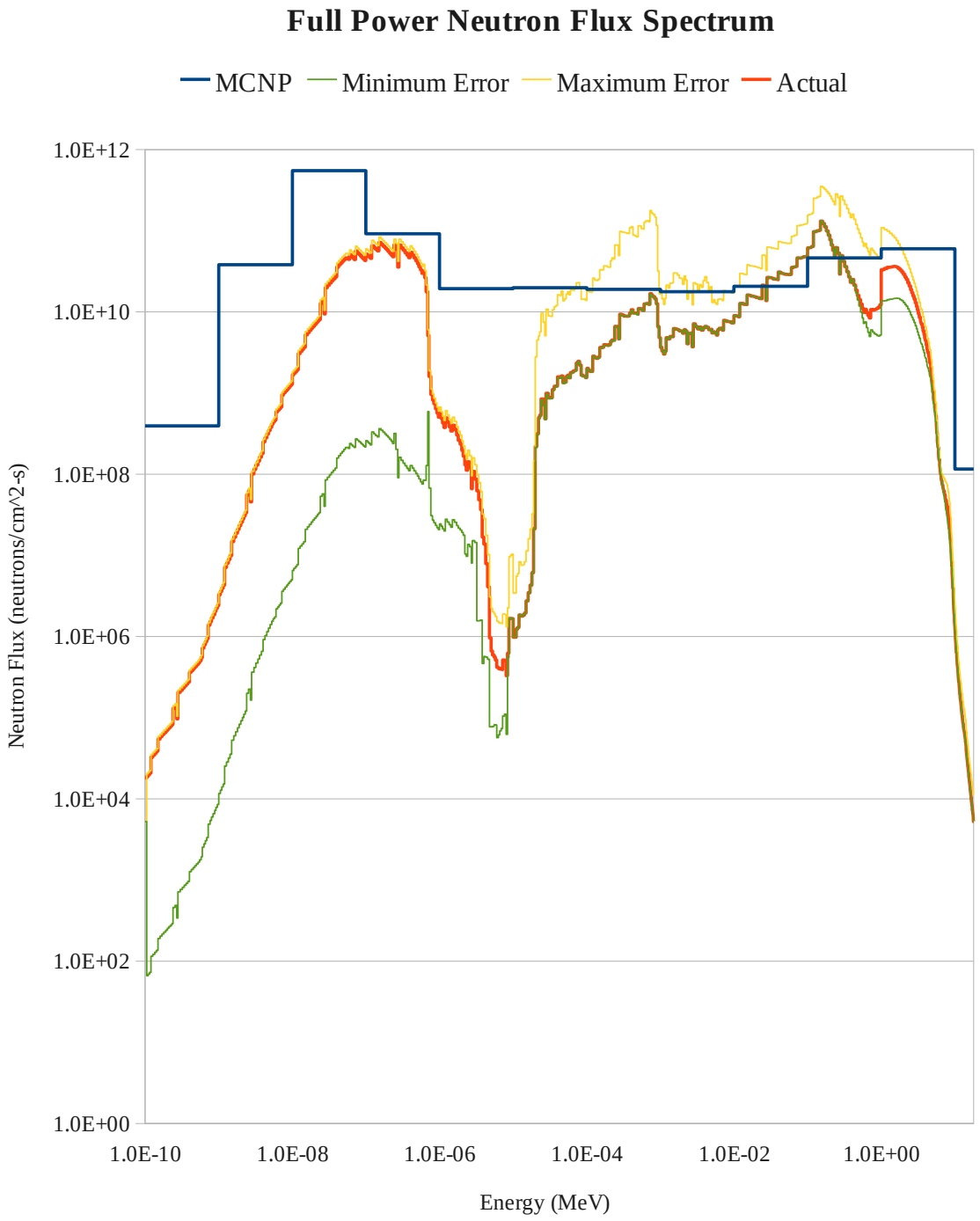

Fig. 6. Full Power neutron flux spectrum for the MSTR.

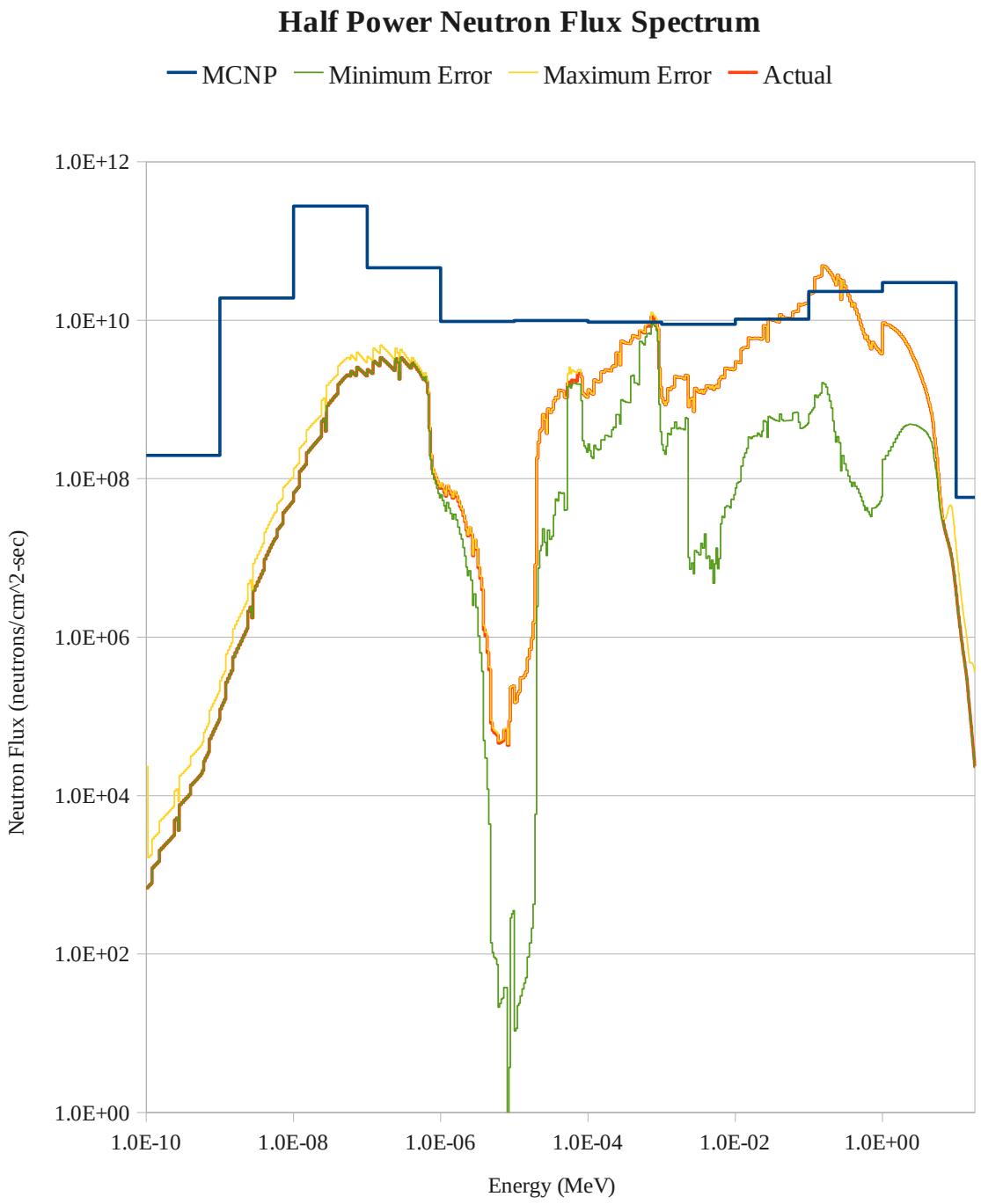

Fig. 7. Half Power neutron flux spectrum for the MSTR.

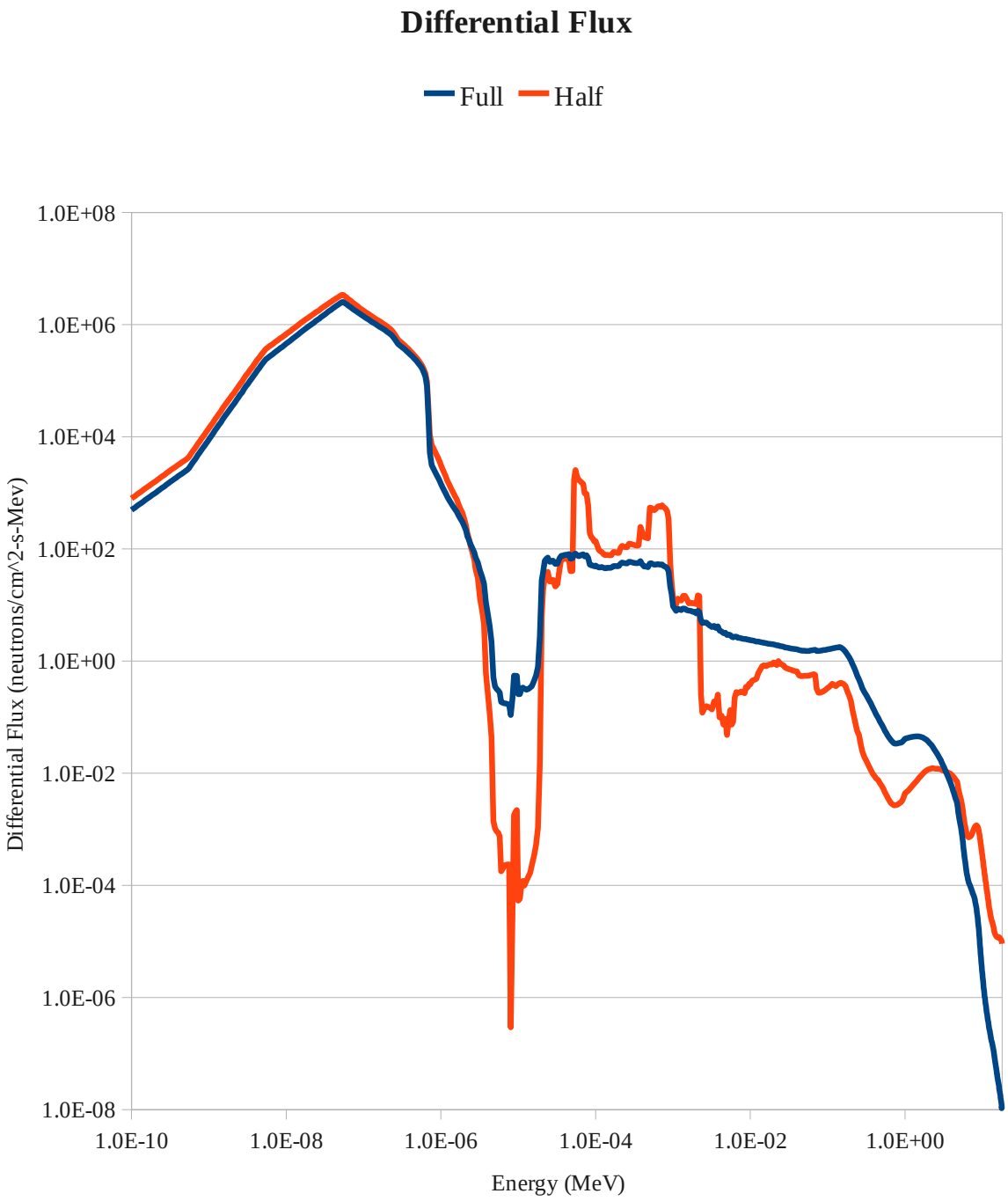

Fig. 8. Differential flux of full and half power

It is expected that the differential flux for full and half power do share some overlap as both are normalized to unity. At low energy the spectrum takes a similar shape, however at energies between 3.5 and 21 eV there is a strong divergence in the spectrum resulting in a significantly greater neutron flux for full power in the region. This fluctuation can also be seen in the integral flux spectrum of Fig. 9, also normalized to unity.

To better quantify the results, spectra were consolidated to three values, namely thermal (<0.625 eV), intermediate (0.625 eV – 100 keV), and fast (>100 keV). These were chosen to match the format already given in the MCNP output file. The output format of the SAND-II program is expressed in differential flux with respect to energy (neutrons/cm^2-s-MeV). To obtain consolidated values, differential flux values from SAND-II were integrated with respect to energy using the energy bounds of thermal, intermediate, and fast for integration and are shown in Table 4 and Table 5. The average error for the consolidated values was obtained from the difference in the integrated maximum and minimum spectra. The average differences between the full power and half power normalized integral fluxes as shown in Fig. 9 are also shown in Table 6. Error values are not shown for the normalized differential flux from Fig. 8 as this information is accurately represented in Table 4 and Table 5 after renormalization to real physical flux values.

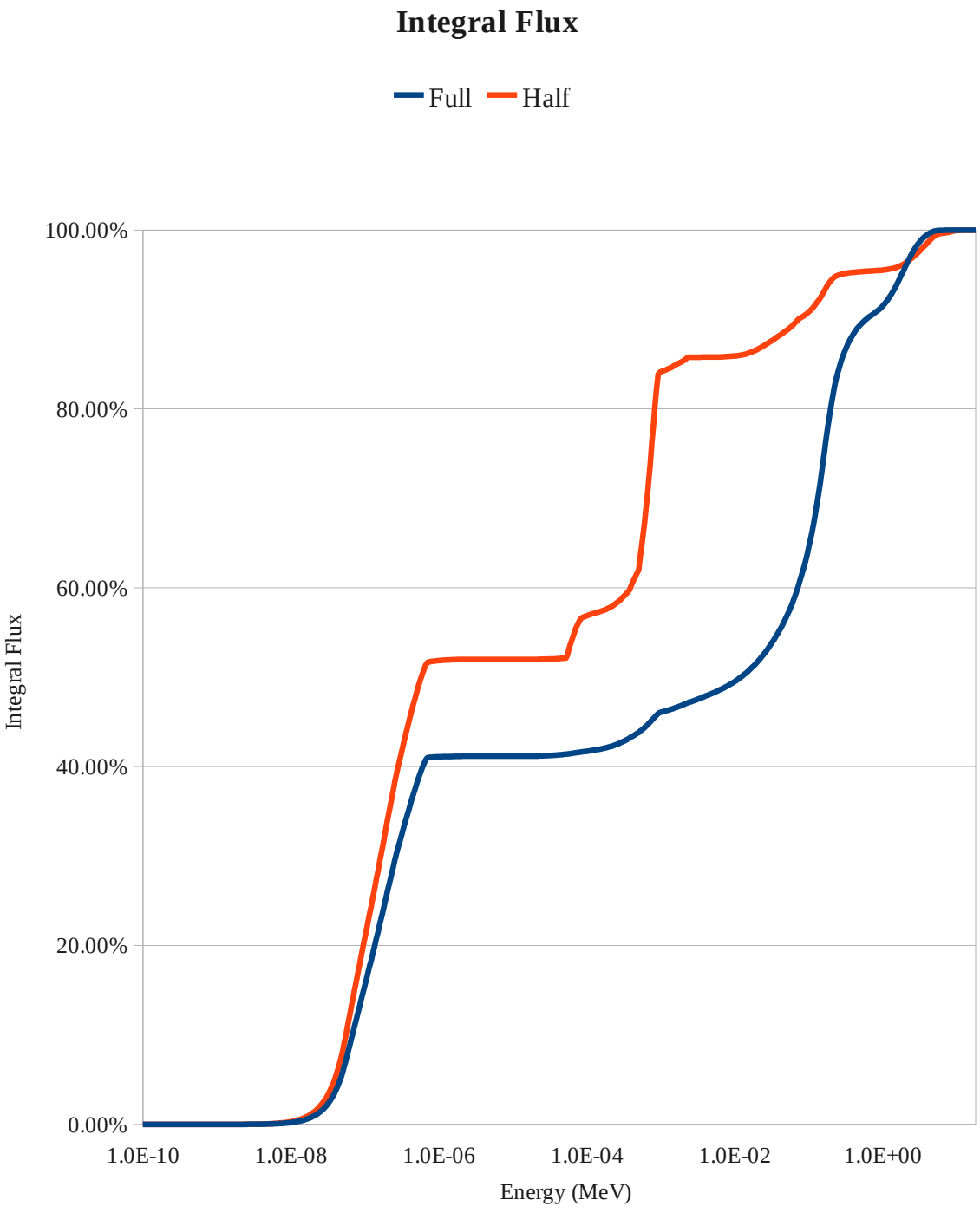

Fig. 9. Integral flux of full and half power

Table 4. Thermal, intermediate, and fast neutron fluxes for full power

Energy	**Flux (neutrons/cm^2-s)**	**Flux Share of total**
Thermal	2.94E+12 ± 1.9E+10	38.993%
Intermediate	1.86E+12 ± 3.7E+10	24.619%
Fast	2.65E+12 ± 3.0E+3	35.152%
Total	7.55E+12 ± 5.7E+10	100.000%

Table 5. Thermal, intermediate, and fast neutron fluxes for half power

Energy	**Flux (neutrons/cm^2-s)**	**Flux Share of total**
Thermal	1.40E+11± 1.2E+08	7.116%
Intermediate	7.44E+11 ± 8.1E+09	37.771%
Fast	1.06E+12 ± 1.7E+05	53.931%
Total	1.97E+12 ± 8.3E+09	100.000%

Table 6. Average normalized integral flux difference

Energy	**Difference**
Thermal	2.18%
Intermediate	22.15%
Fast	2.52%

7. Conclusions

A study of the neutron flux environment of the Missouri S&T research reactor has been completed. The goal of the study was obtain a high resolution neutron spectrum to better predict interactions of neutrons with materials both in and around the reactor core. A detailed MCNP model was used to simulate the neutron flux at a specific location and SAND-II was used in conjunction with experimental data obtained at 100 kW and 200 kW to form a neutron flux spectrum. Cross-section data was taken from the ENDF/B-VII library and 5,000 SAND-II runs were made at each power level to show uncertainty in the flux spectra.

Although there is a discrepancy between the 100 kW and 200 kW neutron flux spectra in the region between 3 eV and 21 eV there is also a sharp sole resonance peak of over 27,411 b around this energy for ^{197}Au, creating a strong likelihood that this discrepancy was the result of a strong dependence on the irradiation of the Au foil. To mask the strong dependence on Au in this region, more foils with equally strong cross-sections in the energy region of interest would need to be irradiated. Another possibility for the discrepancy is the effect of changing temperature on the system. The effective cross-section for the fuel and cladding material could change as temperature rises because the material would thermally expand the material. The fuel plates within each fuel element are designed to curve slightly at room temperature so that expansion would be possible without buckling of the plates. Expansion also occurs in the same direction for all fuel plates so that fuel plates do not expand into each other. As the fuel changes temperature it is possible that the physical distance between the fuel and experiment was changed, bringing the fuel physically closer to the irradiated sample allowed less distance for the pool water to moderate the neutrons. It is also possible that the experiment itself moved in the source holder tube although an effort was made to place the experiment in the

source holder tube in such a way that it would be as close to the core fuel as possible, reducing the amount of water between the experiment and the core. If the experiment had shifted to the other side of the source holder during irradiation, this would place an indeterminate thickness of water between the source holder wall and the experiment changing the moderation of the neutron path to reach the sample.

The similar overall shape of the differential flux (Fig. 8) and integral flux (Fig. 9) normalized to unity show that both sets of independent irradiation data are able to produce similar results leading to the likelihood that the true neutron flux spectrum is accurately represented by the model shown. Further inspection of the differential flux appears to match very consistently in the thermal region, but not as consistently in the intermediate and fast regions. One explanation for the differences is that the contribution of thermal neutrons to the overall activity of an irradiated foil is much greater than that of the intermediate and fast neutrons because of the cross-section differences between these energy ranges. Also clearly visible in the differential flux is the effect of the resonance peak cross-sections in the intermediate neutron energy range. Sharp peaks in the neutron flux in this region are likely due to the drastic changes in cross-section between small changes in neutron energy. As more foils are irradiated, the effects of the resonance peaks will be dampened in the resulting neutron flux spectrum but those effects will never completely disappear. For example, the fuel and cladding materials also have characteristic resonance peaks that can never be eliminated by the irradiation of more foils. The neutron flux is affected in the fuel material before traveling to the point of sample irradiation. This leads to the conclusion that the neutron flux in the thermal region below which resonance effects occur are more than likely very accurate as the full power and half power differential flux values very strongly agree. The intermediate and

fast regions show strong resonance effects that can only be dampened with more foil irradiations.

The resulting neutron flux spectra and uncertainty associated with such spectra represent a great improvement to the previous two group neutron flux model of the MSTR and will be a necessary addition to fully utilize the capabilities of the HSC.

8. Nomenclature

A = activity
A_0 = initial activity
A_s = saturation activity
A_w = atomic weight
C = specific saturation activity
C_f = number of combinations possible
E = energy
F = number of foils
K = composite decay correction factor
K_c = correction factor for nuclide decay during counting
K_i = correction factor for nuclide decay during irradiation
K_w = correction factor for nuclide decay between irradiation and counting
m = mass
M = flux multiplier
N = number of target atoms
N_A = Avogardro's number
n = index variable
P = reactor power
S = net peak area
t = time
T_l = live time of collection (sec)
$T_{1/2}$ = half-life
t_c = detector counting time
t_i = irradiation time
t_w = time between end of irradiation and beginning of detector counting
U_f = conversion factor between μCi and Bq
V = sample mass
y = branching ratio

Greek letters

σ = microscopic cross-section
σ_C = random uncertainty of the specific saturation activity
σ_K = uncertainty of the composite decay correction factor
σ_{Kc} = uncertainty of K_c
σ_{Ki} = uncertainty of K_I
σ_{Kw} = uncertainty of K_w
σ_r = resonance microscopic cross-section
σ_R = random uncertainty in percent
σ_S = uncertainty of total peak area
σ_{sys} = systematic uncertainty
σ_t = thermal microscopic cross-section
$\sigma_{T1/2}$ = uncertainty of half-life
σ_V = uncertainty of the sample mass
σ_y = uncertainty of the branching ratio
$\sigma_{\mu(E)}$ = uncertainty of mass attenuation
σ_ε = uncertainty of the non-attenuated corrected efficiency
$\sigma_{\varepsilon'}$ = uncertainty of the effective efficiency
$\sigma_{\rho\tau}$ = uncertainly of the average sample mass per area
φ = neutron flux
φ_t = thermal neutron flux
φ_r = resonance neutron flux
$\rho\tau$ = average sample mass per area
λ = decay constant
ξ = absolute efficiency
ε = non-attenuated corrected efficiency
ε' = attenuation corrected efficiency
$\mu(E)$ = mass attenuation (cm^2/g) at a gamma of energy E
ν = average neutrons produced per fission

ACKNOWLEDGEMENTS

The authors are grateful to Bill Bonzer and the MSTR staff for assistance with sample handling and experimental preparation and to Stephanie Hurtado for Fortran programming consultation and computational processing time.

REFERENCES

Baum, E.M., Knox, H.D., Miller, T.R., 2002. Chart of the Nuclides, 16th edition, Lockheed Martin.

Canberra Industries, 1998. Genie-2000 Spectroscopy System Customization Tools. Canberra Industries report.

Chadwick, M.B., Oblozinsky, P., Herman, M., 2006. ENDF/B-VII.0: Next Generation Evaluated Nuclear Data Library for Nuclear Science and Technology. Nuclear Data Sheets 107, 2931-3060.

Grant, E.J., personal communication, February 2010.

Khouaja, H., 1995. Neutron Flux Characterization of the Bare Rabbit, Cadmium Rabbit, and Beam Port for the UMRR. UMRR Report, University of Missouri-Rolla, UMRR 95-2.

Kim, C.H., Jang, S., Reece, W.D., 2004. Monte Carlo Modeling of the Texas A&M University Research Reactor. Nuclear Technology 145, 1-10.

King, J.C., personal communication, May 2009.

MacFarlane, R.E. And Muir, D.W., 1994. The NJOY Nuclear Data Processing System. Los Alamos National Laboratory Technical Report, LA-12740-M.

McElroy, W.N., Berg, S., Crockett, T., Hawkins, R.G., September 1967. A Computer-Automated Iterative Method for Neutron Flux Spectra Determination by Foil Activation. Air Force Weapons Laboratory Technical Report, AFWL-TR-67-41.

Nguyen, J., March 2009. Issuance of Renewed Facility License No. R-79 for the Missouri University of Science and Technology Research Reactor, Letter from United States Nuclear Regulatory Commission, NRC ADAMS accession number ML090140511.

Primm, T., personal communication, May 2009.

Shultis, Kenneth and Faw, Richard, 2002. Fundamentals of Nuclear Science and Engineering, Marcel Dekker, New York, pp. 100-119

Straka, M. and Covington, L., 1987. Study of Neutron Physics: Conversion of the University of Missouri-Rolla Reactor to Low-Enriched Fuel. Transactions of the American Nuclear Society 55, 594-595.

Talnagi, J.W., Heimberger, L.A., Aldemir, T., September 1990. Prediction and Measurement of the Neutron Environment in OSURR Experimental Facilities Following Conversion to LEU. Argonne National Laboratory report, ANL/RERTR/TM-18 CONF-9009108

UMRR, April 2008. Annual Progress Report for the University of Missouri-Rolla Reactor Facility. UMRR report, University of Missouri-Rolla, NRC ADAMS accession number ML081300428.

X-5 Monte Carlo Team, 2008. MCNP-A General Monte Carlo N-Particle Transport Code, Version 5. Los Alamos National Laboratory report, LA-CP-03-0245.

VITA

Zachary Kulage was born in St. Louis, MO. In 2005, he received a Reactor Operator license from the Nuclear Regulatory Commission for the Missouri S&T Research Reactor and subsequently received a Senior Reactor Operator license in 2007.

Mr. Kulage served as the president of the Missouri S&T American Nuclear Society (ANS) student chapter from 2007-2008 and was inducted into and served as the secretary of the Missouri S&T student chapter of Alpha Nu Sigma in 2007. In addition, he was also a member of the Missouri S&T student chapter of the American Institute of Chemical Engineers. He completed his B.S. in Nuclear Engineering from Missouri S&T in 2008 and a M.S. in Nuclear Engineering in 2010.